RSC Advances

ROYAL SOCIETY OF CHEMISTRY

www.rsc.org/advances

Cite this: DOI: 10.1039/c0xx00000x

www.rsc.org/xxxxxx

ARTICLE TYPE

Synthesis of lamellar mesostructure aluminophosphate nanoparticles and converting it to a highly efficient adsorbent using ultrasound waves for partial template removal

Babak Seyghali, Mohammad Ali Zanjanchi*, Majid Arvand

Received (in XXX, XXX) Xth XXXXXXXXX 20XX, Accepted Xth XXXXXXXXX 20XX
DOI: 10.1039/b000000x

The partial removal of the structure-directing templates from mesoporous aluminophosphate (AlPO) was studied for developing simple and effective adsorbents for elimination of anionic dye from wastewater. The template species were removed out from the as-synthesized AlPO samples using progressive sequences of sonication of the as-synthesized AlPO in ethanol. The ultrasound-treated AlPO materials were characterized using standard solid-state techniques. The micellar types are altered in the modified samples following the sonication. The as-synthesized and ultrasound-treated AlPOs were examined for adsorption of congo red (CR) as an anionic probe dye. Presence of feasible admicelles in the treated samples provides suitable conditions for establishment of effective interactions between CR and the adsorbent. The products sonicated for 15 min shows the highest adsorption for CR and longer irradiation of ultrasound does not improve it. The obtained adsorption data were well fitted with Langmuir isotherm model based on the calculations performed on the linear form of the equation. A remarkable maximum CR adsorption of 666.3 mg/g was observed for our superior sample. The removal of CR by our AlPO materials follows both pseudo-first order and pseudo-second order reaction kinetics but it is more fitted with the first order based on the calculated correlation coefficients.

Introduction

One of the greatest problems that the world is facing today is that of environmental pollution, increasing with every passing year and causing grave and everlasting damage to the earth.[1] Water pollution can be caused by discharge of wastewater containing dyes, heavy metals and non-degradable chemical compounds from industrial and commercial waste into surface waters. Dyes are considered an objectionable type of pollutant because they are toxic and may significantly affect photosynthetic activity in aquatic life due to reduced light penetration.[2] Numerous techniques have been applied for the removal of pollutant materials from wastewater.[3-7] Among them adsorption is the procedure of choice and gives the best results as it can be used for removal of a variety of pollutants from various contaminated water sources.[6] The design of a potent adsorbent with high capacity has a significant importance which is related to the possibility of establishing various interactions, surface area, pore volume and porosity of the adsorbents.

The discovery of the ordered aluminophosphate (AlPO) molecular sieves by Wilson *et al*. at 1982 announced a rapidly growing of the chemistry of non-silicate microporous solids.[8] The structure of aluminophosphates consisted of alternating tetrahedral AlO_4 and PO_4 connected by shared oxygen atoms.

Department of Chemistry, Faculty of Science, University of Guilan, Rasht, 41335-1914, Iran

* *Corresponding author. Tel.: +98 13 33326643; fax: +98 13 32330066. E-mail addresses: zanjanchi@guilan.ac.ir , mazanjanchi@yahoo.com (M.A. Zanjanchi).*

The most widely observed AlPO structure type (AlPO-n), where n denotes a particular crystalline phase, readily prepared in the presence of a wide variety of organic templates.[9] Also, a variety of organically structure-directed aluminophosphates with anionic chains (one-dimensional), layers (two-dimensional), and frameworks (three-dimensional) have been successfully synthesized.[10,11] These materials are suitable precursors due to of the flexibility of the interlayer space and exciting changes can be made to the layers themselves. Moreover, a change on the hydrophobic/hydrophilic character in the interlayer functional groups is possible.

It would be interesting to study the adsorptive behavior of these layered materials especially the lamellar mesostructured materials with well-defined porous sheet mesostructures. The interlamellar spaces between the Al–O–P layers are occupied by supramolecular templates with hydrogen-bonding possibilities to terminal oxygen atoms in the inorganic layers.[12-14] The supramolecular templates in the synthesis of lamellar AlPOs can be neutral long-chain amine,[15.17] anionic surfactant with a phosphate headgroup,[18] and cationic quaternary alkyl-ammonium surfactant.[19.22] The materials are usually prepared under hydrothermal conditions. In some cases employing ultrasonic waves are beneficial for the synthesis progress.[14]

Tetrapropylammonium hydroxide (TPAOH) mainly used as template in synthesis of AlPO-5,[13,23] ZSM-5,[24,25] silicalite-1[26] and TS-1[27,28] microporous materials. Additionally, the utilization of this chemical for synthesis of a lamellar aluminophosphate as a co-structure directing additive could be valuable.

In the synthesis of mesostructure materials template acts as a structure-directing agent that is essential for control of the frameworks. The pore sizes can be regulated by varying the chain length of the surfactants template in the synthesis

process. These templates generally are removed after the synthesis to generate the genuine porous structure to be used for various applications.[29] Conventionally, the template removal has been carried out by calcinations at elevated temperatures. However, in lamellar mesostructures aluminophosphates because of the template molecules have been located between Al–O–P layers, the calcination process for template removal may cause collapse of the structure. This shows that these products are sensitive to thermal treatment.[16-20,30] Therefore, complete template removal in mesolamellar AlPOs seems to be unlikely. However, there is an alternative procedure for template removal. Solvent extraction is an alternative procedure with less destructive effects for template removal.[15,31] The main disadvantage of this method includes, dependency of the solvent extraction efficiency on the strength of the interaction between organic molecules and the framework, multiple steps, longer time and high consumption of solvent.[29,32, 33]

The aluminophosphate materials have applications is in catalytic processes.[34,35] The lamellar aluminophosphate may also be used as a precursor to synthesis other type of AlPO materials.[36,37] There are reports about the use of aluminophosphates as the adsorbent as well.[38-40] However, to the best of our knowledge the lamellar mesostructured AlPO has not been used as an adsorbent for removal of water pollutants. Investigation which has been conducted in our research laboratory [41] has shown that the partial removal of the surfactant molecules from mesoporous MCM-41 developed simple and effective adsorbents for water remediation. This attractive efficiency is due to establishment of hydrophobic and electrostatic interactions between pollutant and surfactant molecules. Therefore, this procedure which is based on partial removal of template molecules out of the structure could be tested on layered aluminophosphate materials. The ultrasonic treatments can be used as a simple, fast and effective way for partial template removal from these materials.[29,42,43] Our prepared adsorbent by this way will be used for the removal of pollutant from wastewaters, while the lamellar structure is preserved.

With regard to these considerations, in this work we have attempted to demonstrate that the lamellar aluminophosphate (AlPO-L) can be converted to a highly efficient adsorbent by partial removal of the template using a sonication procedure. The congo red dye was utilized as a model pollutant to test the adsorption capability of the samples. The results showed that when the AlPO-L sample was exposed to the ultrasonic waves in an alcoholic solvent for a short period of time, part of the template molecules can be removed without disrupting of mesolamellar structure. Both as-synthesized and sonicated samples were able to absorb the dye molecules. But, the ultrasonic treatment significantly promotes the adsorption capability of the adsorbent.

Experimental section

Reagents and materials

Aluminium triisopropylate ($Al[OCH(CH_3)_2]_3$, AlIP, ≥ 98.0%), ortho-phosphoric acid (H_3PO_4, 85%), tetrapropylammonium hydroxide

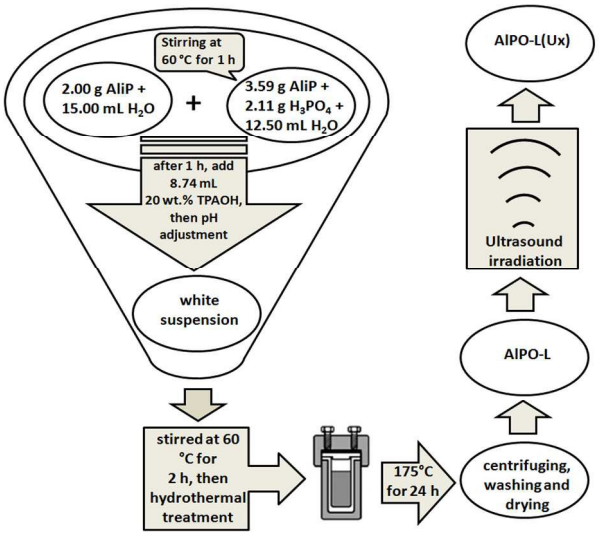

Scheme 1. Schematic presentation of synthesis procedure for preparation of as-synthesized and sonicated aluminophosphate samples

$((C_3H_7)_4N(OH)$, TPAOH, 20% w/v solution in water), cetyltrimethylammonium bromide ($(C_{16}H_{33})N(CH_3)_3Br$, CTAB, ≥ 98.0%), ethanol (C_2H_5OH, ≥ 99.5%) and congo red ($C_{32}H_{22}N_6Na_2O_6S_2$, CR, reagent grade) were obtained from Merck chemical company. All the chemicals were used as received without any further purification.

Synthesis of mesostructure lamellar AlPO

The previously reported procedure in the literature with some modification was used for the synthesis of mesostructure lamellar aluminophosphate.[33] For this purpose 3.59 g AlIP and 2.11 g H_3PO_4 were added into 12.5 mL deionized water and the mixture was stirred at 60 °C for 1 h. Then, 2.00 g CTAB was dissolved in 15.0 mL deionized water and added to the previous mixture. The mixture was stirred again at 60 °C for 1 h. Then, 8.74 mL of 20 wt.% solution of TPAOH was added dropwise into the above mixture. The pH of mixture was adjusted at about 8.0 with adding of 1.0 M HCl. This mixture was stirred at 60 °C for another 2 h and then transferred into a Teflon-lined stainless steel autoclave for hydrothermal treatment. It was heated at a constant temperature of 175 °C for 24 h. The final nominal molar composition of the gel mixture was as follows:

1.00 Al_2O_3 : 1.06 P_2O_5 : 0.32 CTAB : 0.63 TPAOH : 110.13 H_2O

Finally, the autoclave was cooled to room temperature and the resultant precipitate was centrifuged and washed with deionized water and ethanol for several times and dried at 120 °C for 12 h. The final product was designated as AlPO-L. We noticed that addition of TPAOH in lower amounts (just enough to maintain pH at about 8) did not lead to AlPO-L. We called this amorphous product as AlPO-B (Fig. 1).

Ultrasonic treatment procedure

The sonication of the as-synthesized AlPO-L for template removal was carried out in a 7500-S ultrasonic bath (SAIRAN Instrument Company, Iran) with an ultrasound power of 600 W, heating power of 800 W and frequencies of 28 kHz, equipped

with a timer and a temperature controller. For sonication purpose, 0.3 g of AlPO-L was dispersed in 45 ml of ethanol in a baker. Then, the suspension was immersed into water in the ultrasonic bath, and irradiated for 5, to 20 min at temperature of 45 °C. The suspension was stirred during ultrasound irradiation using a mechanical stirrer at the speed of 300 rpm. After sonication, the sample was recovered by centrifugation, washed with ethanol and dried at 80 °C for 5 h. The sonicated samples were designated as AlPO-L(Ux) where U stands for ultrasound-treated samples and x shows time (min) of ultrasound irradiation. The entire steps of the procedure for preparation of AlPO-L(Ux) are depicted in scheme 1.

Characterization

A Philips PW1840 X-ray diffractometer with Cu K_α radiation was used to record the powder XRD patterns of the samples within a 2θ range of 1.5–10°. FT-IR spectra were recorded with Bruker alpha spectrophotometer. The size and morphology of the AlPO-L sample were studied using LEO-1430VP scanning electron microscope. Energy dispersive X-ray analysis (EDX) system (TESCAN-LMU Vega model) was used for the compositional analysis of the sample. For the textural analysis Nitrogen adsorption/desorption experiments were performed at −196 ^{0}C using Belsorp mini II apparatus. Prior to the gas adsorption measurements, the samples were degassed at 120 ^{0}C. Specific surface areas were calculated according to Brunauer–Emmett–Teller (BET) method and the pore size distributions were obtained based on the conventional Barret–Joyner–Halenda (BJH) method. Thermogravimetric analysis (TGA) was performed on a TG (6300 SLL-Nanotechnology company) to estimate the residual amount of the template in the as-synthesized and sonicated AlPO-L samples. The measurements were carried out under static air from room temperature to 500 °C with a heating rate of 10 °C/min.

Adsorption Studies

Congo red (CR) which is a secondary diazo dye with two sulfonate and amine groups and also the hydrophobic aromatic rings (Scheme 2) was used as a model pollutant to investigate the adsorption capability of the as-synthesized and the sonicated AlPO-L samples. For this purpose 15 mg of the adsorbents were added into 50 mL of CR solutions at initial concentration of 200 mg/L. The solution was stirred for definite time periods. To study the adsorption isotherms, experiments were carried out at concentration range of 200-500 mg/L. All the experiments were conducted at natural pH and room

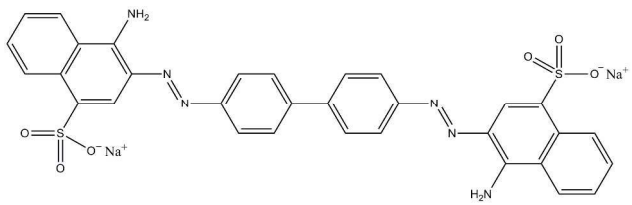

Scheme 2. Chemical structure of congo red.

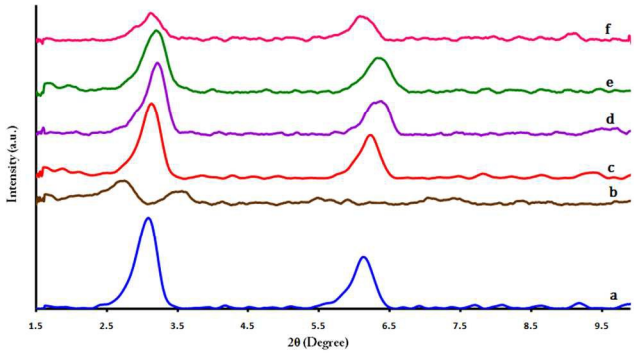

Fig. 1. Low angle XRD patterns of (a) AlPO-L, (b) AlPO-B, (c) AlPO-L(U5), (d) AlPO-L(U10), (e) AlPO-L(U15), (f) AlPO-L(U20).

temperature. The solution and the solid phase were separated by centrifugation and the residual dye concentration was measured by spectrophotometric method. A double beam Shimadzu UV-2100 spectrophotometer was used for the determination of dye concentration at 498 nm. The adsorption capacity of AlPO-L samples was calculated by using the following equation:

$$q = \frac{(C_0 - C_e)V}{m} \quad (1)$$

Where q is the amount of dye adsorbed per unit weight of adsorbent (mg/g); C_0 and C_e are the initial and final concentrations of the dye solution (mg/L), respectively; V is the volume of the dye solution (L); and m is the amount of the sorbent used (g).

Results and discussion

XRD Analysis

The low-angle X-ray diffraction patterns of the as-synthesized and sonicated aluminophosphate materials are shown in Fig. 1. The XRD pattern of AlPO-L (Fig. 1.a) consists of two intense diffraction peaks at 2θ of 3.08° and 6.13° with the d-spacing of 28.7 Å and 14.5 Å, respectively. This reveals the ordered nature of the synthesized AlPO-L. This XRD pattern is quite similar to those reported for mesostructure single lamellar phase aluminophosphates (AlPO-L),[15-22] indicating a successful synthesis of lamellar mesostructure aluminophosphate. The obtained d-space values can be related to interlamellar distances. In some of these reports tetramethylammonium hydroxide (TMAOH) was used as a basic source to adjust the pH value of the starting mixtures and/or for increasing the Al/P ratio to change the structure of the products from lamellar to hexagonal. In our work we replaced TMAOH by TPAOH. We used TPAOH for the two purposes of pH adjustment and also as structure-directing agent. Our investigation showed that, when TPAOH is used as an amount that is just sufficient for pH adjustment, an amorphous phase (AlPO-B) is obtained (Fig. 2b). However, proper amount of TPAOH in the synthesis gel leads to the ordered phase of AlPO-L. This indicates that TPAOH has an essential role in the synthesis of mesostructure AlPO-L. TPAOH as a moderate

Table 1. The 2θ and d-space values for the two characteristics x-ray reflections of as-synthesized and sonicated samples

Sample	2θ (degree)		d-space (Å)	
AlPO-L	3.08	6.13	28.7	14.5
AlPO-L(U5)	3.13	6.22	28.2	14.2
AlPO-L(U10)	3.20	6.33	27.6	14.0
AlPO-L(U15)	3.22	6.37	27.5	13.9

organic lye can act not only as a pH adjuster, but as a co-structure directing agent to increase the order and stability of AlPO-L structure. Kimura *et al.* in their work states that tetramethylammonium cations interact with aluminophosphate oligomers and suppress the polymerization of the aluminophosphate oligomers. [20] Our textural analysis (later in the text) will provide confirmation for function of TPAOH in establishment of meso-structure AlPO-L.

The XRD patterns show that the orders of the mesostructure lamellar structures are preserved for all samples following ultrasounic treatment. However, slight shift to the higher 2θ values (and consequently lower d-spacing) were observed for the sonicated samples (Table 1). This could be attributed to the removal of surfactant template and reduction of interlamellar space.

If the sonication duration exceeds than 15 min, the intensity of the XRD peaks are reduced significantly (Fig. 2f). This may shows partial destruction of the lamellar mesostructure. We did not investigated such samples.

FT-IR spectroscopy

FT–IR spectra of the as-synthesized and ultrasound-treated AlPO-L samples are shown in Fig. 2. The broad band at 3400-3500 cm^{-1} and 1600-1650 cm^{-1} were assigned to the asymmetric O–H stretching and bending vibrations of water molecule, respectively. [39,40,44] The two bands at 2850-2950 cm^{-1} are ascribed to C–H vibrations of $–CH_3$ and $–CH_2–$ carbon chain of the surfactant molecules. The band at 1450-1500 cm^{-1} is due to alkylammonium vibrations of the surfactant and TPAOH molecules. [37,39,41] The bands in the range of 900–1100 cm^{-1} corresponds to P-O stretching vibration of tetrahedral PO_4. [39,44]

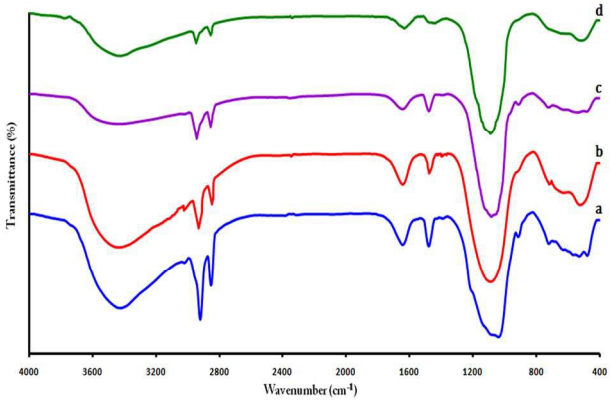

Fig. 2. FTIR spectra of (a) AlPO-L, (b) AlPO-L(U5), (c) AlPO-L(U10) and (d) AlPO-L(U15).

The band at 500-550 cm^{-1} can be attributed to triply degenerate O-P-O bending vibration of PO_4. [39,44] The band at 700-750 cm^{-1}, indicates the stretching vibration of Al-O in combination with P-O. [44] Fig. 3 indicates that the vibrations related to template molecules (2850-2950 cm^{-1} and 1450-1500 cm^{-1}) became weaker as the sonication step proceeded. This clearly verifies that parts of template species have been expelled out of the AlPO-L.

Fig. 3 shows the FT-IR spectra of the effluents of the ultrasound-treated samples and also the FT-IR spectrum of CTAB solution in ethanol (Fig. 3.d) containing the same amount of CTAB that was used in the synthesis process. As can be observed, the spectral characteristics of the effluents are similar with those of CTAB solution which indicates release of CTAB molecules upon sonication. Our previous studies concerning ultrasound template removal from mesoporous MCM-41 [29] revealed that ultrasound irradiation cause micelle disruption and the intact template molecules are released out. Therefore, when AlPO-L sample is sonicated for a certain time part of the template molecules will be removed out from AlPO-L without destruction of its lamellar mesostructure. As a result, longer sonication time will lead to more release of the surfactant molecules into ethanol (Fig.3 a, b and c). It will be seen later that the surfactant molecules remained into the lamellar structure of AlPO-L are responsible for adsorption of the dye molecules. The rate of the adsorption will be related to the amount of the surfactants left inside the AlPO-L structure.

Morphological and compositional analysis

The morphology of the as-synthesized mesostructure AlPO-L was studied by scanning electron microscopy. As it is observed in Fig. 4.a and 4.b the SEM micrographs of AlPO-L consisted of some flake-like and spherical crystalline nanoparticles with dimension range of 30-100 nm. The figures display regions composed of layered structure which somewhat is similar to those are presented in some literature for lamellar aluminophosphate. [19,36,37,45] The spherical aggregated morphology was observed in the lamellar phase with highly condensed AlPO framework. [45] Also, occurrence of holes can be seen in some particles.

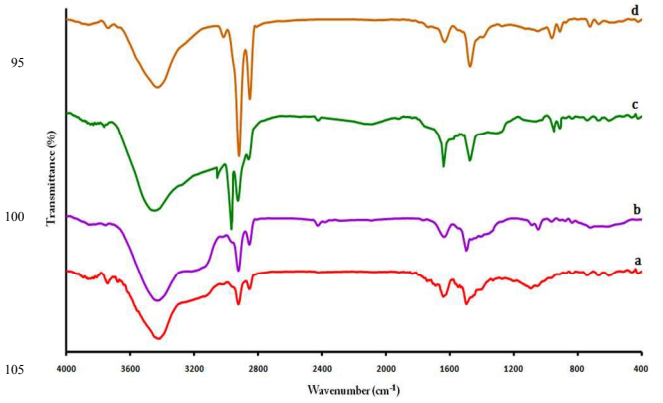

Fig. 3. FTIR spectra of the ethanolic effluent after sonication of (a) AlPO-L(U5), (b) AlPO-L(U10), (c) AlPO-L(U15) and (d) the prepared solution of CTAB in ethanol.

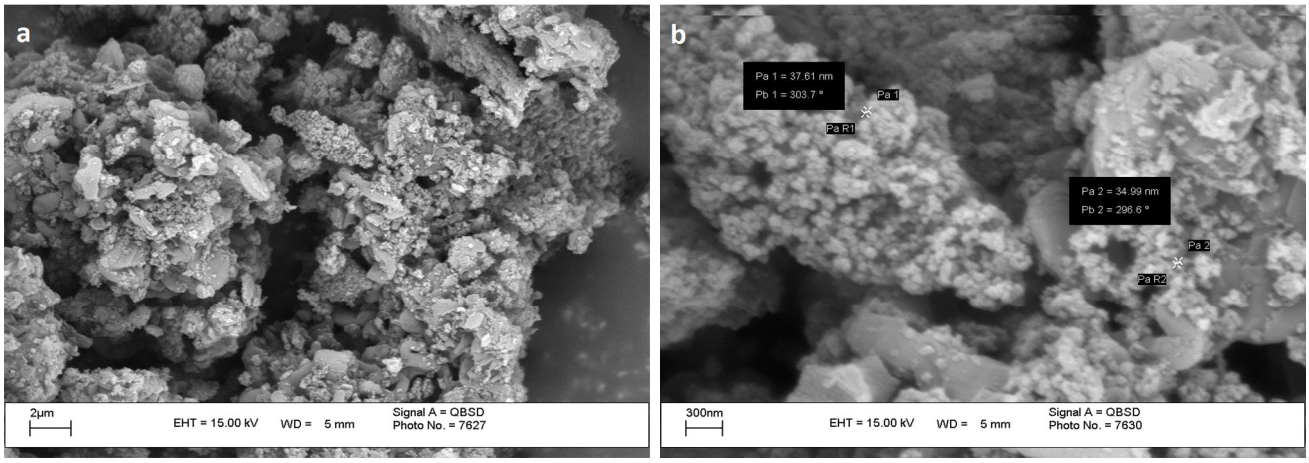

Fig. 4. SEM images of as-synthesized AlPO-L with different magnifications.

The elemental analysis of the as-synthesized AlPO-L was performed using EDX signals recorded at different points (Fig. 5 and Table 2). The table shows that the observed wt.% of Al and P in the lamellar mesostructure sample are 21.4 and 13.5, respectively. When the values of wt.% are divided by their respective atomic weights and normalized (Al + P = 1), [39,46] the observed molecular formula would be $Al_{0.64}P_{0.35}O_{3.32}$. Therefore, the molar ratio of Al and P in the as-synthesized AlPO-L sample is 0.64/0.35. Fig. 5 shows that in addition to the mentioned main elements, the aluminophosphate sample holds some carbon-containing compounds which is due to presence of template molecules.

Table 2. EDX chemical analysis of as-synthesized AlPO-L.

Element	Weight %	Atomic %
Aluminium	21.4	14.9
Phosphorus	13.5	8.2
Oxygen	65.1	76.8

Textural analysis

The results of nitrogen adsorption/desorption isotherms and their respective BJH pore size distributions for AlPO-L, AlPO-L(U5) and AlPO-L(U15) are presented in Figs. 6. All the aluminophosphate samples show isotherms of type IV (according to the IUPAC convention). They show sharp inflation due to capillary condensation, which is characteristic of mesoporous materials. [47] The sample's adsorption-desorption profile indicates presence of H3-type hysteresis loops at high P/P_o, suggesting presence of slit-shaped pores.[47] This is due to lamellar structure of the aluminophosphate samples. The broad BJH pore size distribution suggests wide range of porosity with maximum pore size distributions of 2.5 - 3.1 nm. From the figure it can be deduced that, the mesoporosity and uniformity in the pore size distributions have not been altered upon sonication of the mesolamellar aluminophosphate.

The values of BET surface area, pore volume and pore diameter for the as-synthesized and sonicated samples are shown in Table 3. It is observed that, the value of surface area and pore volume increased successively following longer sonication time. The highest surface area is 311.3 m^2/g which is recorded for AlPO-L(U15) sample.

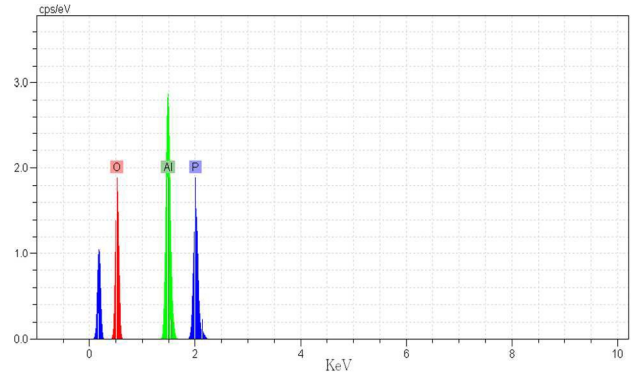

Fig. 5. EDX patterns of as-synthesized AlPO-L.

Thermal analysis

For quantitative determination of the amount of the surfactant expelled out of the sonicated aluminophosphates, the samples were analyzed with thermogravimetric method. The thermograms for the as-synthesized AlPO-L in addition to AlPO-L(U5) and AlPO-L(U15) recorded from 25 to 500 °C are shown in Fig. 7. General features of the thermograms are similar to those reported so far [28, 46] and shows a continuous mass loss. The first step of the weight loss (6.3%) about 100-170 °C is due to desorption of the interlayered and physisorbed water. [18,30,44] A relatively vast two-steps weight loss was observed within the range of 170-470 °C. Previous studies have demonstrated that the CTA^+ species are decomposed mainly in the temperature range of 150 to 360 °C. [33,41,48] Therefore, the weight loss within 170-470 °C will be associated with the thermal decomposition of both CTA and TPA cations. [28] The two-steps weight loss within 170-470 °C may indicate presence of both CTA and TPA in the structure of AlPO-L. This range of weight loss can be used to evaluate the amount of the template removed out in the

Table 3. Textural properties and thermogravimetric data of aluminophosphate samples.

Sample	S_{BET}[a] (m^2/g)	Pore volume[b] (cm^3/g)	Pore diameter[c] (nm)	Template amount[d] (%)
AlPO-L	96.5	0.24	3.09	46
AlPO-L(U5)	193.7	0.42	2.81	34
AlPO-L(U15)	311.3	0.56	2.51	22

[a] *Specific surface area calculated from the linear BET plot.*
[b] *Total pore volume at $P/P_o = 0.98$.*
[c] *Maximum of the size distribution calculated using the BJH method.*
[d] *Weight loss of samples related to the template molecules, based on the thermogravimetric analysis.*

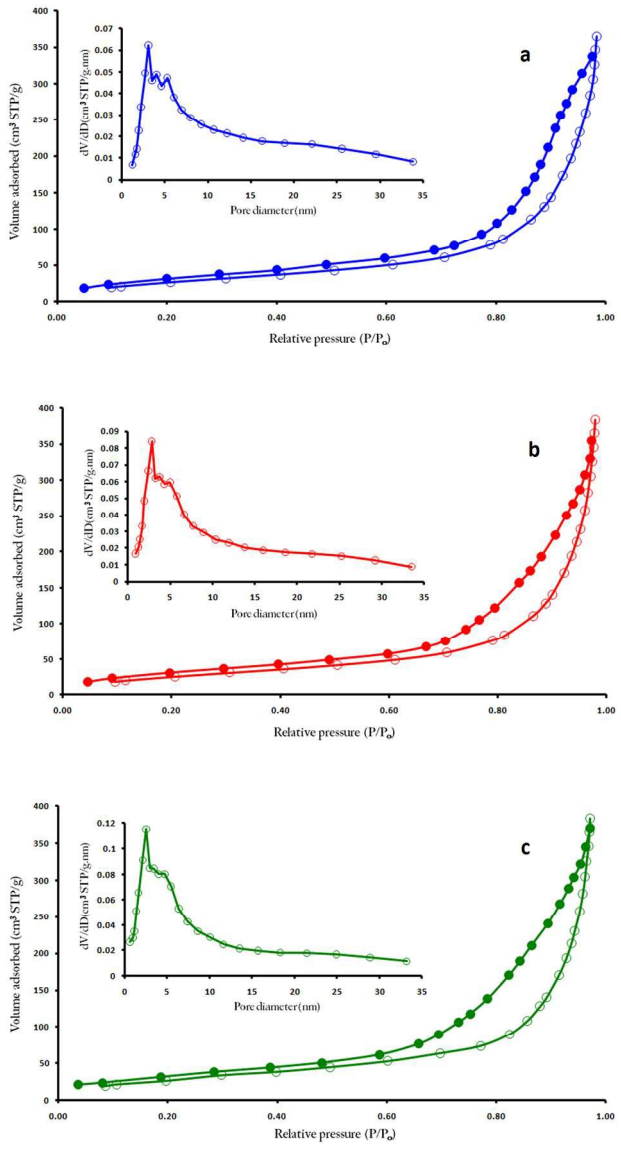

Fig. 6. Nitrogen adsorption–desorption isotherms and corresponding pore-size distribution curves derived from the BJH method (inset) of (a) AlPO-L, (b) AlPO-L(U5) and (c) AlPO-L(U15).

sonicated samples (Fig. 7.b and 7.c).

Based on the thermogravi-metric results, about 46% of the weight of the as-synthesized AlPO-L is due to the template molecules. The amount of template species are about 34% and 22% for AlPO-L(U5) and AlPO-L(U15) samples, respectively (Fig. 7 and Table 3). This means that due to sonication about 12% and 24% of the templates have been removed out from interlamellar spaces of AlPO-L(5) and AlPO-L(15), respectively. This is further confirmation for the partial removal of the template species.

Adsorption studies

The results of congo red adsorption on as-synthesized and sonicated aluminophosphate samples are presented in Fig. 8. It is observed that AlPO-L has the potential for CR removal from aqueous solutions. A dose of 15 mg of AlPO-L is capable to remove more than 82% of CR existed in 50 mL of a 200 mg/L solution of the dye within 90 min. This corresponds to 552.60 mg/g adsorbent capacity. Moreover, this potential is greatly enhanced for the ultrasound-treated AlPO-L. In fact, all of the dye are adsorbed onto AlPO-L(U5), AlPO-L(U10) and AlPO-L(U15) after 90, 50 and 40 min, respectively (more than 662 mg/g adsorption capacity). This indicates that sonication of AlPO-L sample and partial removal of the template species has lead to a considerable improvement in rate of adsorption and capacity of the adsorbent.

Several mechanisms might be involved for the adsorption of CR on our aluminophosphates. The hard-hard acid-base interactions between Al and P in AlPO-L and the nitrogen groups of CR molecules could be a case. Also, hydrogen bonding between H atoms of the hydroxyl groups of AlPO-L and oxygen and/or nitrogen of CR may be involved in adsorption of the dye onto the adsorbent (Fig. 9a). The hydrophobic interactions between alkyl chains of surfactant molecules and apolar part of the dye molecules may contribute for the adsorption (Fig. 9b).[40,41,49] Employing sonication procedure and partial removal of the surfactant cations from interlamellar space of AlPO-L

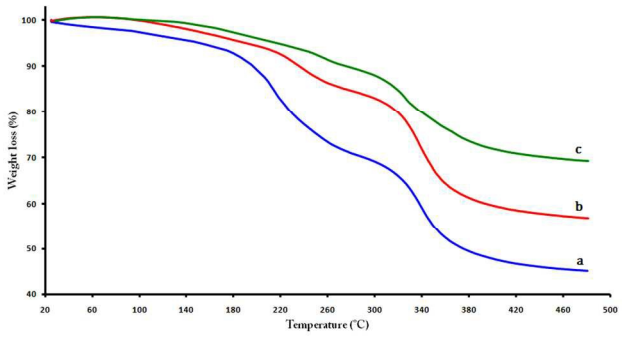

Fig. 7. Thermogravimetric curves of (a) AlPO-L, (b) AlPO-L(U5) and (c) AlPO-L(U15).

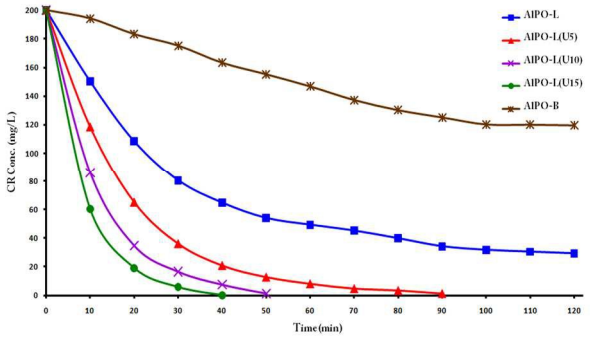

Fig. 8. Adsorption capability of aluminophosphate samples for removal of congo red dye. Adsorbent dose: 15 mg, volume of dye solution: 50 mL, initial dye concentration: 200 mg/L.

without collapse of the lamellar structure will provide an appropriate space for interactions. In addition to that, formation of bilayers of the surfactant molecules (admicelles) may provide an electrostatic interaction between the surfactant positive head and the negatively charged SO_3^- groups of CR. This results in increasing the adsorption capacity of the ultrasound-treated aluminophosphates.

It worth mentioning that in the AlPO-B which TPAOH was added just for pH adjustment the adsorption of dye is much less than AlPO-L (see Fig. 8). This is sensible because AlPO-B did not show the conventional AlPO-L X-ray pattern (Fig. 1.b).

Adsorption Isotherms

Equilibrium data or adsorption isotherms describe how the adsorbate molecules interact with adsorbent particles and determines its maximum adsorption capacity. In the present study, experimental data were evaluated by using two well-known, the Langmuir and Freundlich isotherm equations.

The Langmuir adsorption isotherm assumes that the adsorption takes place at specific homogeneous sites within the adsorbent by monolayer adsorption without any interaction between adsorbed species. [50] The linearized Langmuir equation is represented as follows:

$$\frac{1}{q_e} = \frac{1}{q_m} + \frac{1}{K_L q_m}\frac{1}{C_e} \qquad (2)$$

Where q_e is the adsorbed amount of the dye, C_e is the equilibrium concentration of the dye in solution, q_m is the maximum amount of adsorption which complete monolayer coverage on the adsorbent surface (mg/g), and K_L is the Langmuir constant (L/mg) indicating the affinity for the binding of adsorbates. The essential features of the Langmuir isotherm can be expressed in terms of a dimensionless constant called separation factor or equilibrium parameter (R_L) which is defined by Eq. (3).

$$R_L = \frac{1}{1+K_L C_m} \qquad (3)$$

Where C_m is the maximum initial dye concentration (mg/L). The values of this parameter are basically classified into four groups, indicating the shape of the isotherm, in which $R_L>1$ is unfavourable, $R_L=1$ is linear, $0<R_L<1$ is favourable, and $R_L=0$ is irreversible.

The Freundlich isotherm describes a non-ideal adsorption that takes place on heterogeneous surfaces and suggests that adsorption is multilayer. [50] This isotherm is explained by the following equation:

$$\log q_e = \log K_F + \frac{1}{n}\log C_e \qquad (4)$$

Where q_e is the amount of dye adsorbed per unit of adsorbent (mg/g), C_e is the concentration of dye solution at adsorption equilibrium (mg/L), K_F (mg/g) and n are the Freundlich isotherm constants relating adsorption capacity and adsorption intensity. Higher the 1/n value more favorable is the adsorption.

The adsorption constants of CR onto AlPO-L, AlPO-L(U5), AlPO-L(U10) and AlPO-L(U15) were calculated and listed in Table 4. The values of the correlation coefficients (R^2) for the Langmuir isotherm (R^2 > 0.99) suggests that the aluminophosphate samples are well fitted with this model and the R_L values obtained for all samples ($0 < R_L < 1$) confirm the favorable process of adsorption. Therefore, it can be concluded that, dye adsorption on AlPO-L samples is a homogeneous and monolayer process. The Freundlich model is less capable of describing the adsorption equilibrium due to the lower value of R^2. The maximum monolayer adsorption capacity of AlPO-L for CR is 666.67 mg/g as calculated from Langmuir model which increased to 1000 mg/g for AlPO-L(U15). This clearly confirms the great

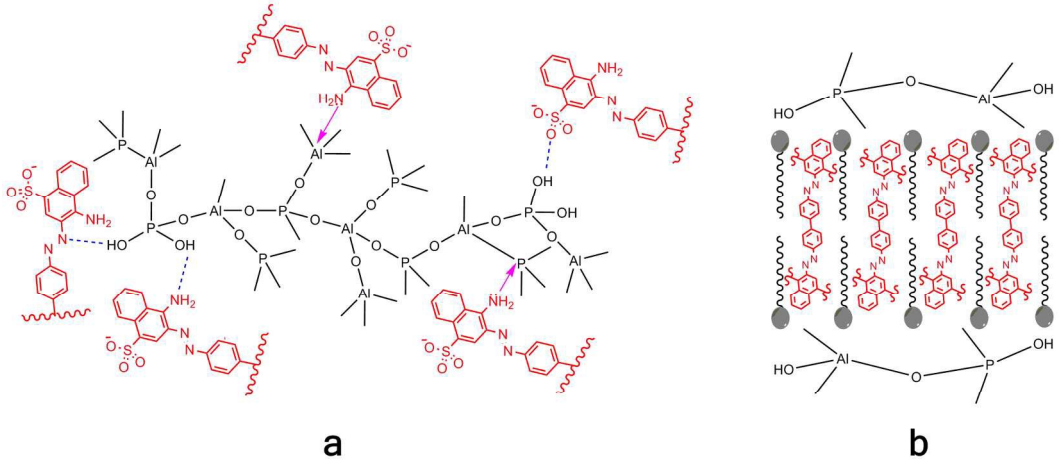

Fig. 9. Pictorial representations for adsorption of CR on AlPO samples: (a) acid-base interactions and hydrogen bonding; (b) hydrophobic interactions.

Table 4. Isotherm parameters for adsorption of CR on aluminophosphate samples

Sample	Langmuir isotherm				Freundlich isotherm		
	q_m (mg/g)	K_L (L/mg)	R_L	R^2	K_F ($mg^{(1-1/n)}/g\ L^{1/n}$)	1/n	R^2
AlPO-L	666.67	0.1613	0.0122	0.9916	440.25	0.0669	0.9692
AlPO-L(U5)	833.33	0.2973	0.0067	0.9917	655.09	0.0524	0.9850
AlPO-L(U10)	909.09	0.3928	0.0051	0.9921	661.61	0.0626	0.9649
AlPO-L(U15)	1000.0	0.8330	0.0024	0.9936	755.61	0.0505	0.9735

potential of our mesostructure lamellar AlPO-L adsorbents for the removal of CR molecules from wastewaters. The improved efficiency the of the ultrasound-treated sample (AlPO-L(U15)) shows success of our thought. Table 4 shows that the Langmuir K_L constant increases with increasing sonication time that can verify the formation of favorable position in the interlamellar space of AlPO-L.

Adsorption kinetics

The adsorption kinetics provides views about adsorptive interaction pathways, rate of dye removal and controls the efficiency of the process. Among the several kinetics models, the pseudo first-order and pseudo second-order models which are based on chemical reactions order have been widely used. [51,52] Pseudo first-order model proposed by Lagergren can be expressed as follows:

$$\frac{dq_t}{dt} = k_1(q_e - q_t) \quad (5)$$

At boundary conditions t=0 to t=t and q=0 to q=q_t, the integration of Eq. (6) gives:

$$\ln(q_e - q_t) = \ln q_{e1} - k_1 t \quad (6)$$

Where q_e and q_t is the amount of dye adsorbed per unit of adsorbent (mg/g) at equilibrium and at any time t, k_1 is the pseudo-first order rate constant (1/min), and t is the contact time (min). The adsorption rate constant (k_1) were calculated from the slope of the plot of ln (q_e-q_t) against t.

The pseudo-second-order model is given as Eq. (7):

$$\frac{dq_t}{dt} = k_2(q_e - q_t)^2 \quad (7)$$

Integrating this equation for the boundary conditions (t=0 to t=t and q=0 to q=q_t), gives rearranged linear form:

$$\frac{t}{q_t} = \frac{1}{k_2 {q_{e2}}^2} + \frac{1}{q_{e2}} t \quad (8)$$

Where q_{e2} is theoretical equilibrium adsorption capacity and k_2 is the pseudo-second order rate constant (g/mg.min). A plot of t/q_t against t provides second order adsorption rate constants q_{e2} and k_2 values from the slopes and intercepts, respectively.

The kinetics parameters of both models for the as-synthesized and sonicated samples are presented in Table 5. The K and $q_{e,\ cal}$ values are calculated from the linear plots of t/q versus t (Fig. 10). The correlation coefficients are very high for both models, suggesting that the adsorption process may follows from both kinetic models. However, the correlation coefficients for pseudo-first-order are higher and the experimental q_e ($q_{e,exp}$) are closer to the calculated q_e ($q_{e,cal}$) values based on the first-order model. Therefore, the pseudo-first order kinetic model well fitted the experimental data. Table 5 also shows that the rate constant increased with increasing sonication time; so that k_1 and k_2 for AlPO-L(U15) is about 2.9 and 4.7 times faster than that of the as-synthesized AlPO-L, respectively. Hence, it is concluded that the ultrasonic treatment has had a positive impact on the capability of AlPO-L for CR adsorption.

It should be noted that in most literature when the dye adsorption process comply with the pseudo-second order model, the adsorption is very fast at first, and then it is more slowly due to the saturation of adsorption sites. [53,54] However, in case of AlPO-L sample most of dye molecules are adsorbed

Table 5. Kinetic parameters for adsorption of CR on aluminophosphate samples.

Sample	$q_{e,\ exp}$ (mg/g)	Pseudo first-order model			Pseudo second-order model		
		K_1 (1/min)	$q_{e,\ cal}$ (mg/g)	R^2	K_2 (g/mg.min)	$q_{e,\ cal}$ (mg/g)	R^2
AlPO-L	552.60	4.12×10^{-2}	556.63	0.9927	4.29×10^{-5}	769.23	0.9839
AlPO-L(U5)	662.03	5.67×10^{-2}	660.24	0.9992	7.20×10^{-5}	833.33	0.9932
AlPO-L(U10)	662.30	8.68×10^{-2}	660.50	0.9991	11.43×10^{-5}	833.33	0.9972
AlPO-L(U15)	666.30	11.86×10^{-2}	665.07	0.9997	20.09×10^{-5}	769.23	0.9987

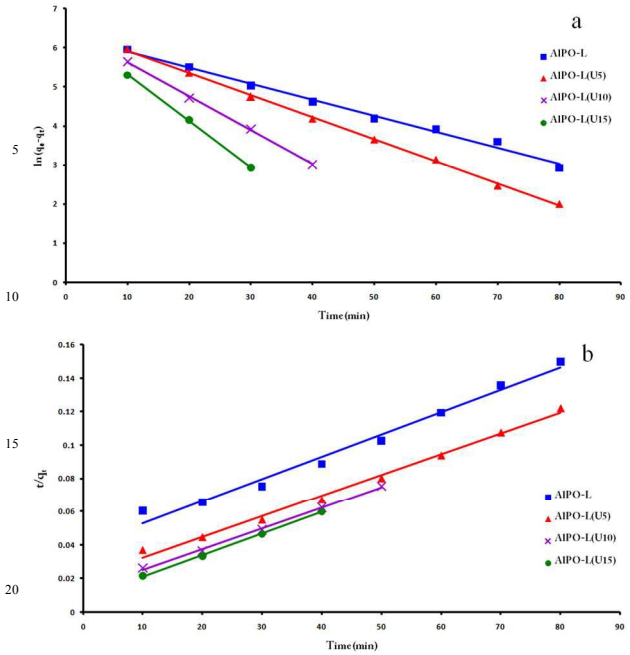

Fig. 10. Kinetic models for adsorption of CR onto AlPO-L samples. (a) pseudo-first-order and (b) Pseudo-second-order rate equations.

through hydrophobic interactions in interlamellar space which the dye removal is a relatively gradual process due to the micelle accumulation and restriction of space. In the sonicated samples due to expansion of space for hydrophobic interactions and also probable involvement of electrostatic interactions the dye adsorption process proceeded more quickly.

Conclusion

Partial elimination of the structure-directing surfactant molecules from the ordered mesoporous aluminophsphate leads to develop highly efficient adsorbent for the removal of congo red from aqueous solution. The as-synthesized AlPO-L adsorb congo red due to micellar interactions with the dye molecules. The capacity of this adsorbent was improved by expelling out some of the template molecules out of the pore layers. Different amounts of the surfactant molecules were taken out of the pores of AlPO-L using successive ultrasound irradiation of the materials. The AlPO-L sample irradiated for 15 min shows best result. This increase in adsorption capacity may be attributed to the formation of the surfactant bilayers which provide suitable conditions for establishment of both hydrophobic and electrostatic interactions between CR and the solid. Longer ultrasound treatment lowered the structural ordering of AlPO-L and was not studied further. The Langmuir isotherm is a suitable model to describe adsorption of CR onto AlPO-L and the modified samples. A remarkable Q_{max} of about 1000 mg/g was observed for AlPO-L(U15). The high loading capacity observed for AlPO-L and for AlPO-L samples succeeded controlled and optimized elimination of the template from it, may leads to develop potential adsorbents for anionic species remediation in certain applications.

Acknowledgment

We gratefully acknowledge the Research Department of University of Guilan for supporting this work.

Notes and references

1 M.K. Hill, *Cambridge University Press,* United Kingdom, 2010.
2 R.M. Christie (Ed.), *CRC Press, Woodhead Publishing Limited, Cambridge,* England, 2007.
3 V.K. Gupta, Suhas, *J. Environ. Manag.* 2009, **90,** 2313.
4 N. Bolong, A.F. Ismail, M.R. Salim, T. Matsuura, *Desalination* 2009, **239**, 229.
5 Y.L. Pang, A.Z. Abdullah, S. Bhatia, *Desalination* 2011, **277,** 1.
6 A.Ahmad, S.H. Mohd-Setapar, S.C. Chuo, A. Khatoon, W.A. Wani, R. Kumar, M. Rafatullah, *RSC Adv.* 2015, **5**, 30801.
7 M. Vakili, M. Rafatullah, B. Salamatinia, A.Z. Abdullah, M.H. Ibrahim, K.B. Tan, Z. Gholami, P. Amouzgar, *Carbohyd. Polym.* 2014, **113**, 115.
8 S.T. Wilson, B.M. Lok, C.A. Messina, E.R. Cannan, E.M. Flanigen, *J. Am. Chem. Soc.* 1982, **104,** 1146.
9 N. Rajic, V. Kaucic, N.Z Logar, *John Wiley & Sons Inc.* 2011.
10 W. Yan, J. Yu, Y. Li, Z. Shi, R. Xu, *J. Solid State Chem.* 2002, **167,** 282.
11 S. Oliver, A. Kuperman, A. Lough, G.A. Ozin, *Chem. Mater.* 1996, **8,** 2391.
12 K.O. Kongshaug, H. Fjellvåg, K.P. Lillerud, *Micropor. Mesopor. Mater.* 1999, **32,** 17.
13 H.O. Pastore, S. Coluccia, L. Marchese, *Annu. Rev. Mater. Res.* 2005, **35,** 351.
14 L. Peng, J. Yu, J. Li, Y. Li, R. Xu, *Chem. Mater.* 2005, **17,** 2101.
15 K. Sarkar, A. Bhaumik, *J. Porous. Mater.* 2008, **15,** 445.
16 A. Sayari, I. Moudrakovski, J.S. Reddy, *Chem. Mater.* 1996, **8,** 2080.
17 A. Sayari, *Stud. Surface Sci. Catal.* 1997, **105,** 37.
18 M. Fröba, M. Tiemann, *Chem. Mater.* 1998, **10,** 3475.
19 Y. Z. Khimyak, J. Klinowski, *Chem. Mater.* 1998, **10,** 2258.
20 T. Kimura, Y. Sugahara, K. Kuroda, *Chem. Mater.* 1999, **11,** 508.
21 Y. Z. Khimyak, J. Klinowski, *Phys. Chem. Chem. Phys.* 2000, **2,** 5275.
22 Z.Y. Yuan, T.H. Chen, J.Z. Wang, H.X. Li, *Mater. Chem. Phys.* 2001, **68,** 110.
23 J.P. Zhai, Z.K. Tang, Z.M. Li, I.L. Li, F.Y. Jiang, P. Sheng, X. Hu, *Chem. Mater.* 2006, **18,** 1505.
24 A.A. Rownaghi, F. Rezaei, J. Hedlund, *Micropor. Mesopor. Mater.* 2012, **151,** 26.
25 T. Xue, L. Chen, Y.M. Wang, M.Y. He, *Micropor. Mesopor. Mater.* 2012, **156,** 97.
26 O. Prokopova, B. Bernauer,. M. Frycova, P. Hrabanek, A. Zikanova, M. Kocirik, *J. Phys. Chem.* 2013, **C 117,** 1468.
27 L. Chen, Y.M. Wang , M.Y. He, *Mater. Res. Bull.* 2011, **46,** 698.
28 J.H. Zhang, M.B. Yue, X.N. Wang, D. Qin, *Micropor. Mesopor. Mater.* 2015, **217,** 96.
29 S. Jabariyan, M.A. Zanjanchi, *Ultrason. Sonochem.* 2012, **19,** 1087.
30 J.O. Perez, R.B. Borade, A. Clearfield, *J. Mol. Struct.* 1998, **470,** 221.
31 M. Tiemann, M. Schulz, C. Jäger, M. Fröba, *Chem. Mater.* 2001, **13,** 2885.
32 S. Hitz, R. Prins, *J. Catal.* 1997, **168,** 194.
33 J. Yu, A. Wang, X.Li, J. Tan, Y. Hu, *Mater. Lett.* 2007, **61,** 2620.
34 M.P. Kapoor, A. Raj, *Appl. Catal. A: Gen.* 2000, **203,** 311.
35 G. Liu, Z. Wang, M. Jia, X. Zou, X. Zhu, W. Zhang, D. Jiang, *J. Phys. Chem.* 2006, **B 110,** 16953.
36 N. Venkatathri, S.G. Hegde, V. Ramaswamy, S. Sivasanker, *Micropor. Mesopor. Mater.* 1998, **23,** 277.
37 G.A.V. Martins, H.O. Pastore, *Micropor. Mesopor. Mater.* 2008, **116,** 131.
38 T.Y. Ma, X.J. Zhang, Z.Y. Yuan, *J. Phys. Chem.* 2009, **C 113,** 12854–.
39 S.K. Das, M.K. Bhunia, A.Bhaumik, *Micropor. Mesopor. Mater.* 2012, **155,** 258.
40 C. Kannan, K. Muthuraja, M.R. Devi, *J. Hazard. Mater.* 2013, **244–245,** 10.
41 A. Ariapad, M.A. Zanjanchi, M. Arvand, *Desalination* 2012, **284,** 142.
42 J.S. Jin, L. Cao, G.X. Su, C.Y. Xu, Z.T. Zhang, X.H. Gao, H.H. Liu, H.T. Liu, *Ultrason. Sonochem.* 2014, **21,** 1688.
43 J. González-Rivera, J. Tovar-Rodríguez, E. Bramanti, C. Duce, I. Longo, E. Fratini, I.R. Galindo-Esquivel, C. Ferrari, *J. Mater. Chem. A* 2014, **2,** 7020.
44 Á.B. Sifontes, G. González, L.M. Tovar, F.J. Méndez, M.E. Gomes, E.

Cañizales, G. Niño-Vega, H. Villalobos, J.L. Brito, *Mater. Res. Bull.* 2013, **48,** 730.
45 T. Kimura, Micropor. *Mesopor. Mater.* 2005, **77,** 97.
46 S.K. Das, M.K. Bhunia, A.K. Sinha, A. Bhaumik, *ACS Catal.* 2011, **1,** 493.
47 K.S.W. Sing, D.H. Everett, R.A.W. Haul, L. Moscou, R.A. Pierotti, J. Rouquerol, T. Siemieniewska, *Pure Appl. Chem.* 1985, **57,** 603.
48 F. Kleitz, W. Schmidt, F. Schüth, *Micropor. Mesopor. Mater.* 2003, **65,** 1.
49 S. Liu, Y. Ding, P. Li, K. Diao, X. Tan, F. Lei, Y. Zhan, Q. Li, B. Huang, Z. Huang, *Chem. Engin. J.* 2014, **248,** 135.
50 R.T. Yang, *John Wiley & Sons Inc.* New York, 2003.
51 A. Witek-Krowiak, *Chem. Engin. J.* 2011, **171,** 976.
52 Y.S. Ho, *J. Hazard. Mater.* 2006, **B136,** 681.
53 E. Alver, A.Ü. Metin, *Chem. Engin. J.* 2012, **200–202,** 59.
54 M. Abbas, M. Trari, *Process Saf. Environ. Prot.* 2015 **98,** 424.

- Ultrasound irradiation alters micellar arrangement in lamellar aluminophosphate improving its adsoption capability.